

**Determining the Presence of Ordering in Ternary
Semiconductor Alloys Grown by Molecular Beam Epitaxy**

by Wendy L. Sarney and Stefan P. Svensson

ARL-TN-0520

January 2013

NOTICES

Disclaimers

The findings in this report are not to be construed as an official Department of the Army position unless so designated by other authorized documents.

Citation of manufacturer's or trade names does not constitute an official endorsement or approval of the use thereof.

Destroy this report when it is no longer needed. Do not return it to the originator.

Army Research Laboratory

Adelphi, MD 20783-1197

ARL-TN-0520

January 2013

Determining the Presence of Ordering in Ternary Semiconductor Alloys Grown by Molecular Beam Epitaxy

Wendy L. Sarney and Stefan P. Svensson
Sensors and Electron Devices Directorate, ARL

REPORT DOCUMENTATION PAGE			Form Approved OMB No. 0704-0188		
Public reporting burden for this collection of information is estimated to average 1 hour per response, including the time for reviewing instructions, searching existing data sources, gathering and maintaining the data needed, and completing and reviewing the collection information. Send comments regarding this burden estimate or any other aspect of this collection of information, including suggestions for reducing the burden, to Department of Defense, Washington Headquarters Services, Directorate for Information Operations and Reports (0704-0188), 1215 Jefferson Davis Highway, Suite 1204, Arlington, VA 22202-4302. Respondents should be aware that notwithstanding any other provision of law, no person shall be subject to any penalty for failing to comply with a collection of information if it does not display a currently valid OMB control number. PLEASE DO NOT RETURN YOUR FORM TO THE ABOVE ADDRESS.					
1. REPORT DATE (DD-MM-YYYY) January 2013		2. REPORT TYPE Final		3. DATES COVERED (From - To) July 31, 2012	
4. TITLE AND SUBTITLE Determining the Presence of Ordering in Ternary Semiconductor Alloys Grown by Molecular Beam Epitaxy			5a. CONTRACT NUMBER		
			5b. GRANT NUMBER		
			5c. PROGRAM ELEMENT NUMBER		
6. AUTHOR(S) Wendy L. Sarney and Stefan P. Svensson			5d. PROJECT NUMBER		
			5e. TASK NUMBER		
			5f. WORK UNIT NUMBER		
7. PERFORMING ORGANIZATION NAME(S) AND ADDRESS(ES) U.S. Army Research Laboratory ATTN: RDRL-SEE-I 2800 Powder Mill Road Adelphi, MD 20783-1197			8. PERFORMING ORGANIZATION REPORT NUMBER ARL-TN-0520		
9. SPONSORING/MONITORING AGENCY NAME(S) AND ADDRESS(ES)			10. SPONSOR/MONITOR'S ACRONYM(S)		
			11. SPONSOR/MONITOR'S REPORT NUMBER(S)		
12. DISTRIBUTION/AVAILABILITY STATEMENT Approved for public release; distribution unlimited.					
13. SUPPLEMENTARY NOTES					
14. ABSTRACT Some ternary semiconductor alloys spontaneously order during growth. We observe this phenomenon in some alloys grown for infrared (IR) applications by molecular beam epitaxy (MBE). Ordering can affect not only the crystal structure, but also important optical and electronic properties that ultimately affect a material's suitability for IR device applications. It is important to be aware of the presence of ordering, which is not usually detectable by the standard (004) x-ray diffraction (XRD) measurements typically used as a simple measurement of film quality.					
15. SUBJECT TERMS Transmission electron microscopy, molecular beam epitaxy, diffraction, semiconductors					
16. SECURITY CLASSIFICATION OF:			17. LIMITATION OF ABSTRACT UU	18. NUMBER OF PAGES 18	19a. NAME OF RESPONSIBLE PERSON Wendy L. Sarney
a. REPORT Unclassified	b. ABSTRACT Unclassified	c. THIS PAGE Unclassified			19b. TELEPHONE NUMBER (Include area code) (301) 394-5761

Contents

List of Figures	iv
1. Introduction	1
2. Motivation and Army Interest	1
3. Identification of CuPt Ordering	3
4. Identification of Rotation-induced Compositional Ordering	7
5. Conclusion	9
6. References	10
List of Symbols, Abbreviations, and Acronyms	11
Distribution List	12

List of Figures

Figure 1. Lattice constant vs. bandgap diagram of common III-V semiconductors.....	2
Figure 2. Simulated diffraction pattern of zinc-blende ternary crystal.....	4
Figure 3. Partial unit cell of a ternary alloy with CuPt ordering.....	5
Figure 4. Simulated diffraction pattern of zinc-blende ternary crystal with CuPt ordering.	6
Figure 5. Diffraction pattern of InAsSb with rotation-induced ordering.....	8
Figure 6. InAsSb/InAs SL with rotation-induced ordering within the InAsSb layers.....	9

1. Introduction

Under certain conditions, some ternary semiconductor alloys spontaneously order during growth. At the U.S. Army Research Laboratory (ARL), we observe this phenomenon in some alloys grown for infrared (IR) applications by molecular beam epitaxy (MBE). Ordering can affect not only the crystal structure, but also important optical and electronic properties that ultimately affect a material's suitability for IR device applications. It is important to be aware of the presence of ordering, which is not usually detectable by the standard (004) x-ray diffraction (XRD) measurements typically used as a simple measurement of film quality.

2. Motivation and Army Interest

One common example of ordering seen in many semiconductor alloys is copper platinum (CuPt) type ordering. In the case of an AB_xC_{1-x} ternary, where A is a group III and B and C are group-Vs, the two group V atoms are ordered on the $\{\bar{1}11\}$ sublattice planes. Other groups, for example, conducted extensive studies of the effect of CuPt ordering on the reduction of bandgap of gallium indium phosphide (GaInP) (1). The difficulty in detecting and controlling ordering led to a large discrepancy in measured values reported from different authors (2).

Over the last several years, ARL's III-V program has investigated quantum well infrared photodetector (QWIP) structures type II strained layer superlattices (Type II-SLS), and type II quantum dot infrared photodetector (QDIP) superlattices (SL). The Type II-SLS is the focus of most recent research activity and funding within the IR community. This is because it has been presumed that no direct bandgap III-V material could reach longwave infrared (LWIR) wavelengths.

Indium arsenide antimonide (InAsSb) has the smallest direct bandgap among the III-V compound semiconductors (3), as shown in figure 1. Recent work at ARL, in collaboration with Stony Brook University, shows a larger bowing parameter for InAsSb than previously believed and therefore the random alloy InAsSb can reach LWIR bandgaps without resorting to SLs (4). Upon further development, this will provide a III-V analog to direct bandgap mercury cadmium telluride (HgCdTe), with the benefits of higher quantum efficiencies (QEs) and higher absorption relative to the SL approach. In addition, the bulk InAsSb did not suffer from the growth challenges associated with a multi-interface approach, nor did it contain gallium (Ga), which is the source of the low minority carrier lifetimes that plague Ga-based type-II SLs (5). A bulk

approach likely would have numerous advantages over a SLS approach, with less inefficiency and transport burdens, and stronger absorption.

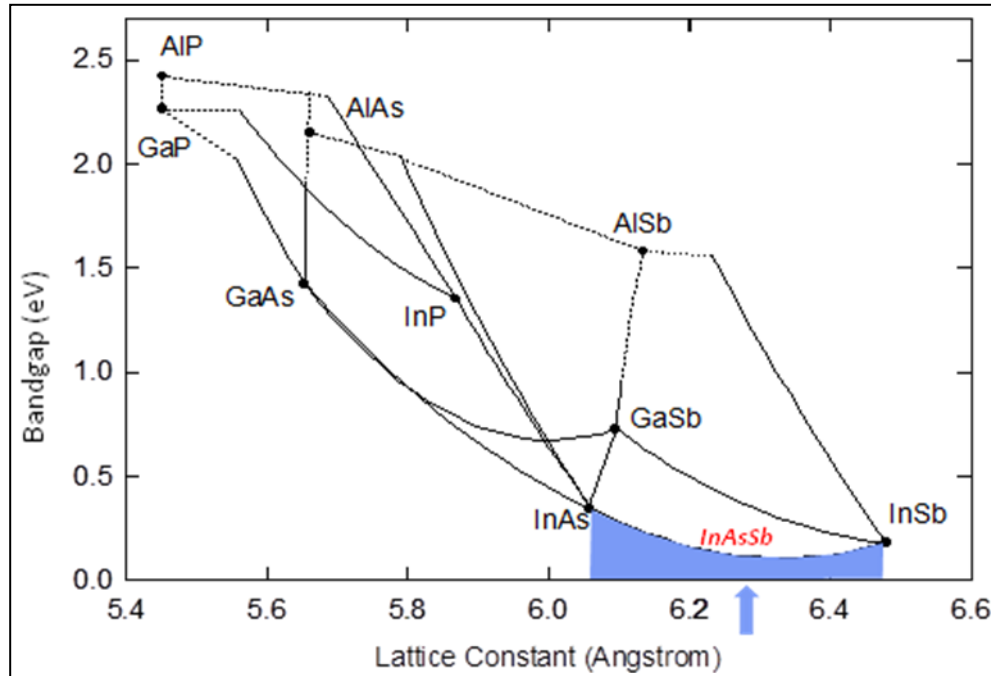


Figure 1. Lattice constant vs. bandgap diagram of common III-V semiconductors.

To develop InAsSb alloys for LWIR, we needed to be certain that the low bandgaps were inherent to the unstrained alloy and were not reliant on a hard-to-control property such as ordering. Prior work by other labs indicated that ordering was common in InAsSb and could reduce the bandgap. For instance, Wei and Zunger predicted that this effect could theoretically lower the bandgap in perfectly ordered InAsSb even to the semi-metallic regime (6). Kurtz et al. observed bandgap narrowing experimentally (7).

The ARL approach is unique in that, with Stony Brook University, we developed graded buffer layers that allow the growth of unstrained, unrelaxed InAsSb alloys having native lattice constants over a range of compositions on both indium antimonide (InSb) and gallium antimonide (GaSb) substrates (8). Transmission electron microscopy (TEM) results indicate that this unstrained material does not have ordering. Therefore, disordered InAsSb with its native lattice constant is a viable candidate material for low-temperature, LWIR detector applications.

3. Identification of CuPt Ordering

We use InAsSb as an illustrative example, but the following treatment is valid for any zinc-blende cubic ternary alloy exhibiting CuPt ordering.

The intensity of the diffraction spots is typically reduced to the square of the structure factor

$$I_{hkl} \propto |F_{hkl}|^2 \quad (1)$$

First, we consider the disordered case, which has a zinc-blende structure with the space group $T^2_d - F43m$. The space group of a crystal refers to the three-dimensional symmetry of the smallest repeatable unit of the crystal. The atoms are in the positions listed below:

$$\begin{aligned} \text{In: } & \left(\frac{1}{4} \frac{1}{4} \frac{1}{4} \right) \left(\frac{3}{4} \frac{3}{4} \frac{1}{4} \right) \left(\frac{3}{4} \frac{1}{4} \frac{3}{4} \right) \left(\frac{1}{4} \frac{3}{4} \frac{3}{4} \right) \\ \text{As or Sb: } & (000) \left(\frac{1}{2} \frac{1}{2} 0 \right) \left(\frac{1}{2} 0 \frac{1}{2} \right) \left(0 \frac{1}{2} \frac{1}{2} \right) \end{aligned}$$

The general equation for the structure factor is

$$F_{hkl} = \sum_i f_i e^{2\pi i(hx_i + ky_i + lz_i)} \quad (2)$$

where x , y , and z are the positions of the atoms in the unit cell and h , k , and l are integer Miller Indices.

Therefore, for the completely disordered case:

$$F_{hkl} = f_{In} e^{\frac{\pi}{2}(h+k+l)} + (0.5f_{As} + 0.5f_{Sb}) [1 + e^{i\pi(h+k)} + e^{i\pi(k+l)} + e^{\pi i(h+l)}] \quad (3)$$

Substituting in the atomic positions gives:

$$F_{hkl} = 0 \text{ for } hkl \text{ mixed}$$

$$F_{hkl} = 4[0.5(f_{As} + 5f_{Sb}) + f_{In}] \text{ for } h+k+l = 4n; \quad n : \text{integer, } hkl \text{ even}$$

$$F_{hkl} = 4[0.5(f_{As} + 5f_{Sb}) - f_{In}] \text{ for } h+k+l = 2(2n+1); \quad n : \text{integer, } hkl \text{ even}$$

$$F_{hkl} = 4[0.5(f_{As} + 5f_{Sb}) - if_{In}] \text{ for } hkl \text{ odd}$$

A crystal with a disordered, zinc-blende structure and the structure factor given in equation 3 has a diffraction pattern shown in figure 2 for the [110] zone axis.

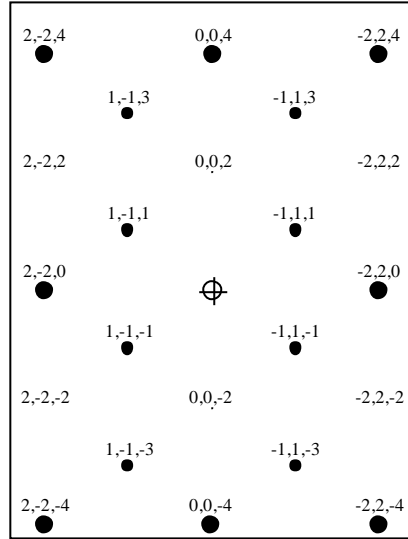


Figure 2. Simulated diffraction pattern of zinc-blende ternary crystal.

If CuPt ordering is present, then the As and Sb atoms are arranged on the $\{\bar{1}11\}$ group-V sublattice planes. This size of the unit cell needed to describe the ordered material is double that needed for the disordered case. The atoms are arranged as shown in figure 3. The In atoms are represented by the red spheres, the As by the black spheres, and the Sb by the blue spheres. The positions for a unit cell of size $2a$ are listed below:

$$\begin{aligned}
 \text{In:} \quad & \left(\frac{111}{888}\right) \left(\frac{151}{888}\right) \left(\frac{171}{888}\right) \left(\frac{133}{888}\right) \left(\frac{173}{888}\right) \left(\frac{115}{888}\right) \left(\frac{175}{888}\right) \left(\frac{155}{888}\right) \left(\frac{137}{888}\right) \left(\frac{177}{888}\right) \\
 & \left(\frac{313}{888}\right) \left(\frac{317}{888}\right) \left(\frac{331}{888}\right) \left(\frac{335}{888}\right) \left(\frac{353}{888}\right) \left(\frac{357}{888}\right) \\
 & \left(\frac{511}{888}\right) \left(\frac{515}{888}\right) \left(\frac{533}{888}\right) \left(\frac{537}{888}\right) \left(\frac{551}{888}\right) \left(\frac{555}{888}\right) \left(\frac{573}{888}\right) \left(\frac{577}{888}\right) \\
 & \left(\frac{711}{888}\right) \left(\frac{713}{888}\right) \left(\frac{715}{888}\right) \left(\frac{771}{888}\right) \left(\frac{717}{888}\right) \left(\frac{753}{888}\right) \left(\frac{757}{888}\right) \left(\frac{775}{888}\right) \\
 \text{As:} \quad & (000) \left(\frac{11}{44}0\right) \left(0\frac{11}{44}\right) \left(\frac{11}{22}0\right) \left(\frac{1}{2}0\frac{1}{2}\right) \left(0\frac{11}{22}\right) \left(\frac{3}{4}0\frac{1}{4}\right) \left(\frac{1}{4}0\frac{3}{4}\right) \\
 & \left(\frac{111}{424}\right) \left(0\frac{33}{44}\right) \left(\frac{33}{44}0\right) \left(\frac{311}{442}\right) \left(\frac{313}{424}\right) \left(\frac{131}{442}\right) \left(\frac{113}{244}\right) \left(\frac{131}{244}\right)
 \end{aligned}$$

$$\text{Sb: } \begin{pmatrix} 1 & 0 & 0 \\ 2 & & \end{pmatrix} \begin{pmatrix} 0 & 1 & 0 \\ 2 & & \end{pmatrix} \begin{pmatrix} 0 & 0 & 1 \\ 2 & & \end{pmatrix} \begin{pmatrix} 1 & 0 & 1 \\ 4 & 4 & \end{pmatrix} \begin{pmatrix} 0 & 1 & 3 \\ 4 & 4 & \end{pmatrix} \begin{pmatrix} 0 & 3 & 1 \\ 4 & 4 & \end{pmatrix} \begin{pmatrix} 1 & 3 & 0 \\ 4 & 4 & \end{pmatrix} \begin{pmatrix} 1 & 1 & 1 \\ 4 & 4 & 2 \end{pmatrix} \begin{pmatrix} 1 & 1 & 1 \\ 2 & 4 & 4 \end{pmatrix} \\ \begin{pmatrix} 1 & 1 & 1 \\ 2 & 2 & 2 \end{pmatrix} \begin{pmatrix} 3 & 0 & 3 \\ 4 & 4 & \end{pmatrix} \begin{pmatrix} 3 & 1 & 0 \\ 4 & 4 & \end{pmatrix} \begin{pmatrix} 1 & 1 & 3 \\ 4 & 2 & 4 \end{pmatrix} \begin{pmatrix} 3 & 1 & 1 \\ 4 & 2 & 4 \end{pmatrix} \begin{pmatrix} 3 & 3 & 1 \\ 4 & 4 & 2 \end{pmatrix} \begin{pmatrix} 1 & 3 & 3 \\ 2 & 4 & 4 \end{pmatrix}$$

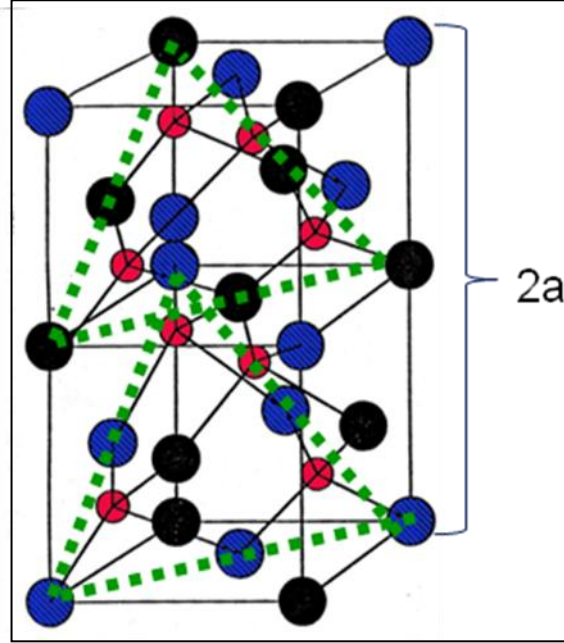


Figure 3. Partial unit cell of a ternary alloy with CuPt ordering.

For simplicity, we neglect the contribution from In, since the positions of the In atoms are the same in the disordered lattice as they are in the ordered lattice.

Therefore, using the atomic positions for the group V elements in equation 2 gives

$$F_{hkl} = f_{As} \left[1 + e^{\frac{\pi i}{2}(h+k)} + e^{\frac{\pi i}{2}(k+l)} + e^{\pi i(h+k)} + e^{\pi i(h+l)} + e^{\pi i(k+l)} + e^{\frac{\pi i}{2}(3h+l)} + e^{\frac{\pi i}{2}(h+3l)} + e^{\frac{\pi i}{2}(h+2k+l)} + e^{\frac{\pi i}{2}(3k+3l)} \right. \\ \left. + e^{\frac{\pi i}{2}(3h+3k)} + e^{\frac{\pi i}{2}(3h+k+2l)} + e^{\frac{\pi i}{2}(3h+2k+3l)} + e^{\frac{\pi i}{2}(h+3k+2l)} + e^{\frac{\pi i}{2}(2h+k+3l)} + e^{\frac{\pi i}{2}(2h+3k+l)} \right] + \\ f_{Sb} \left[e^{\pi i(h)} + e^{\pi i(k)} + e^{\pi i(l)} + e^{\pi i(h+k)} + e^{\pi i(h+l)} + e^{\pi i(k+l)} + e^{\frac{\pi i}{2}(h+l)} + e^{\frac{\pi i}{2}(k+3l)} + e^{\frac{\pi i}{2}(3k+l)} + e^{\frac{\pi i}{2}(h+3k)} + \right. \\ \left. e^{\frac{\pi i}{2}(h+k+2l)} + e^{\frac{\pi i}{2}(2h+k+l)} + e^{\pi i(h+k+l)} + e^{\frac{\pi i}{2}(3h+3l)} + e^{\frac{\pi i}{2}(3h+k)} + e^{\frac{\pi i}{2}(h+2k+3l)} + e^{\frac{\pi i}{2}(3h+2k+l)} + e^{\frac{\pi i}{2}(3h+3k+2l)} + e^{\frac{\pi i}{2}(2h+3k+3l)} \right] \quad (5)$$

This expression becomes

$$F_{hkl} = \left[f_{As} + f_{Sb} e^{\frac{i\pi}{2}(h+l)} \right] \left[1 + e^{\frac{\pi}{2}(h+k)} + e^{\frac{\pi}{2}(k+l)} + e^{\pi(h+k)} + e^{\pi(h+l)} + e^{\pi(k+l)} + e^{\frac{\pi}{2}(3h+l)} + e^{\frac{\pi}{2}(h+3l)} + e^{\frac{\pi}{2}(h+2k+l)} + e^{\frac{\pi}{2}(3k+3l)} + e^{\frac{\pi}{2}(3h+3k)} + e^{\frac{\pi}{2}(3h+k+2l)} + e^{\frac{\pi}{2}(3h+2k+3l)} + e^{\frac{\pi}{2}(h+3k+2l)} + e^{\frac{\pi}{2}(2h+k+3l)} + e^{\frac{\pi}{2}(2h+3k+l)} \right] \quad (6)$$

In terms of a unit cell of side a, the superstructure spots of type $\left\{ \frac{1}{2} \frac{\bar{1}}{2} \frac{1}{2} \right\}$ have a structure factor

$$F = 16(f_{As} - f_{Sb}) \quad (7)$$

for the perfectly ordered case. If we take into account the ordering parameter, S, where S=0 defines a completely disordered alloy and S=1 defines complete ordering, equation 7 is modified as

$$F = 16S(f_{As} - f_{Sb}) \quad (8)$$

A zinc-blende ternary alloy with CuPt ordering has a diffraction pattern, shown in figure 4 for the [110] zone axis.

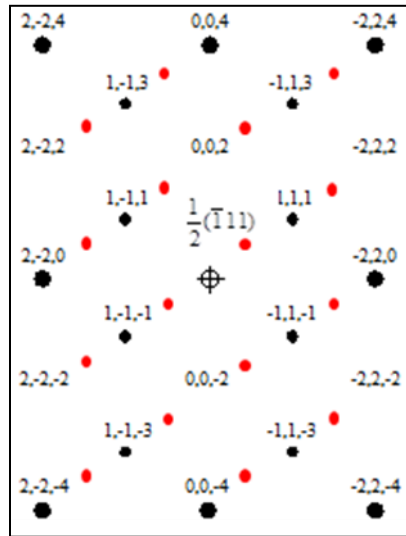


Figure 4. Simulated diffraction pattern of zinc-blende ternary crystal with CuPt ordering.

4. Identification of Rotation-induced Compositional Ordering

Compositional ordering along the growth direction can also be induced during MBE growth of any compound semiconductor composed of more than two elements on the different lattice sites. This originates from the source-substrate geometry and the substrate rotation used to even out thickness variations across the wafer. Unlike the parameter thickness, composition cannot be averaged at a given location in the film. Instead, as we have published in prior studies, at any arbitrary point at a finite radial distance from the rotation center, a compositional SL may form with a band-edge amplitude that increases towards the edge of the sample (9, 10).

For instance, again using the example of InAsSb, this rotation-induced effect results in a SL of $\text{InAs}_{1-x}\text{Sb}_x/\text{InAs}_{1-y}\text{Sb}_y$ with a period, W , equal to $G/R*60$, where G is the growth rate in $\text{\AA}/\text{sec}$ and R is the rotation speed in revolutions per minute. The difference between x and y will increase from zero at the rotation center of the sample to larger values towards the edge. Rotation-induced ordering must be considered since it changes the bandgap of the alloy. To minimize this effect, all samples processed for devices should be prepared from material taken near the rotation center, where the SL effect disappears.

Rotation-induced ordering lengthens the unit cell along the growth direction, leading to the presence of additional diffraction spots in normally forbidden locations along the $[001]$ direction. An example is shown in figure 5.

When samples are imaged using a chemically sensitive reflection, the SL becomes visible. One example of a chemically sensitive reflection is the (002) spot, which is not normally chosen since its structure factor is weaker than that of the standard (004) spot. For this same reason, most standard x-ray rocking curves are collected for the (004) reflection. The (002) reflection is chemically sensitive because its structure factor is largely dependent on the difference between the group V atomic scattering factors, i.e.,

$$F_{002} \propto 4x(f_{As} - f_{Sb}). \quad (9)$$



Figure 5. Diffraction pattern of InAsSb with rotation-induced ordering.

This is opposed to the (004) reflection, which is dependent on the sum of the group III and group V elements.

$$F_{004} = F_{220} = 4[xf_{As} + (1-x)f_{Sb} + f_m] \quad (10)$$

where x is the As mole fraction.

An example is shown in figure 6, which is an $\text{InAs}_{0.72}\text{Sb}_{0.28}/\text{InAs}$ SL. Rotation-induced ordering in the $\text{InAs}_{0.72}\text{Sb}_{0.28}$ layers leads to the fine period SL within the ternary layers. This, in turn, creates a “superlattice within a superlattice” effect.

It is very easy to miss the presence of rotation-induced ordering, since a nonconventional diffraction spot must be used to make it visible.

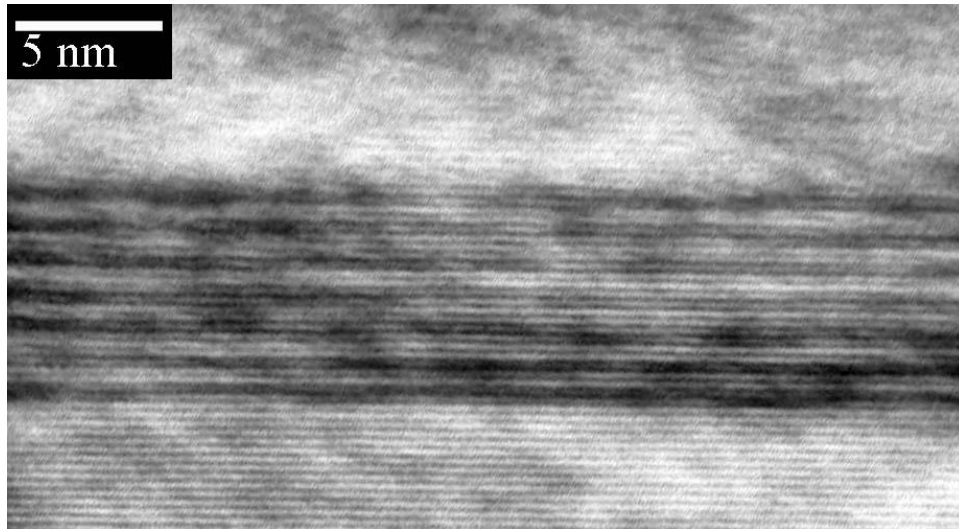


Figure 6. $\text{InAsSb}/\text{InAs}$ SL with rotation-induced ordering within the InAsSb layers.

5. Conclusion

In this report, we discuss two common cases of ordering in semiconductor alloys grown by ARL for IR applications. The treatment in the report serves as an illustrative example, as well as a reference for calculating structural factors of other alloys. Since ordering can affect the electronic and optical properties of alloys, it is important to fully characterize a material to determine the presence and extent of ordering.

6. References

1. Gomyo, A.; Iobgayashi, K.; Kawata, S.; Hino, I.; Suzuki, T.; Yuasa, T. *J Crystal Growth* **1987**, *77*, 367.
2. Stringfellow, G. B.; Lindquist, P. F.; Burmeister, R. A. *J. Electron. Mater.* **1972**, *1*, 437.
3. Thompson, A. G.; Wolley, J. C. *Can. J. Phys.* **1967**, *45*, 225.
4. Wang, D.; Lin, Y.; Donetsky, D.; Shterengas, L.; Kipshidze, G.; Belenky, G.; Sarney, W. L.; Hier, H.; Svensson, S. P. *Proc. SPIE* **2012**, 8353–38.
5. Svensson, S. P.; Donetsky, D.; Wang, D.; Hier, H.; Crowne, F. J.; Belenky, G. *J. Crystal Growth* **2011**, *334*, 103.
6. Wei, S.-H.; Zunger, A. *Appl. Phys. Lett.* **1991**, *58*, 2684.
7. Kurtz, S. R.; Dawson, L. R.; Biefeld, R. M.; Follstaedt, D. M.; Doyle, B. L. *Phys. Rev* **1992**, *B46*, 1909.
8. Sarney, W. L.; Svensson, S. P.; Hier, H.; Kipshidze, G.; Donetsky, D.; Wang, D.; Shterengas, L.; Belenky, G. Structural and Luminescent Properties of Bulk InAsSb. *J. Vac. Sci. Technol.* **2012**, *B30* (2).
9. Svensson, S. P.; Uppal, P. N.; Gill, D. M. *J. Vac. Sci. Technol.* **1994**, *B14*, 2192.
10. Sarney, W. L.; Svensson, S. P. *Materials Characterization* **2007**, *58*, 284.

List of Symbols, Abbreviations, and Acronyms

ARL	U.S. Army Research Laboratory
CuPt	copper platinum
Ga	gallium
GaInP	gallium indium phosphide
GaSb	gallium antimonide
HgCdTe	mercury cadmium telluride
InAsSb	indium arsenide antimonide
InSb	indium antimonide
IR	infrared
LWIR	longwave infrared
MBE	molecular beam epitaxy
QDIP	quantum dot infrared photodetector
QEs	quantum efficiencies
QWIP	quantum well infrared photodetector
SL	superlattice
TEM	transmission electron microscopy
Type II-SLS	type-II strained layer superlattice
XRD	x-ray diffraction

NO. OF COPIES	ORGANIZATION
1 ELEC	ADMNSTR DEFNS TECHL INFO CTR ATTN DTIC OCP 8725 JOHN J KINGMAN RD STE 0944 FT BELVOIR VA 22060-6218
1	US ARMY RSRCH DEV AND ENGRG CMND ARMAMENT RSRCH DEV & ENGRG CTR ARMAMENT ENGRG & TECHNLOGY CTR ATTN AMSRD AAR AEF T J MATTS BLDG 305 ABERDEEN PROVING GROUND MD 21005-5001
1	US ARMY INFO SYS ENGRG CMND ATTN AMSEL IE TD A RIVERA FT HUACHUCA AZ 85613-5300
1	US GOVERNMENT PRINT OFF DEPOSITORY RECEIVING SECTION ATTN MAIL STOP IDAD J TATE 732 NORTH CAPITOL ST NW WASHINGTON DC 20402
3	US ARMY RSRCH LAB ATTN IMNE ALC HRR MAIL & RECORDS MGMT ATTN RDRL CIO LL TECHL LIB ATTN RDRL SEE I W SARNEY ADELPHI MD 20783-1197

TOTAL: 7 (1 ELEC, 6 HCS)